Instability Analysis of Grid-Connected Inverters During Low-voltage-ride Through Process

Qijin Yang[1], Yuanda Liu[1], Yong Han[1], Chunbao Zou[1], Cheng Luo[2]

[1] Yunnan Energy Investment Co., Ltd. of Three Gorges Corporation, Kunming 650000, Yunnan, China;

[2] TBEA Xi'an Electric Technology Co., Ltd, Xi'an 710100, Shaanxi, China

Corresponding author: Cheng Luo, 18829235749@163.com

Speaker: Cheng Luo, 18829235749@163.com

Abstract

During the low voltage ride-through (LVRT) process, it is found that grid-connected inverters may experience instability. The reason is that when outputting the reactive current according to the grid-voltage dip value, the large grid impedance may lead to the root of the characteristic expression moving outside the unit circle. A low-pass filter (LPF) with a designed cut-off frequency is proposed to be used with the voltage magnitude detection module. It is revealed that LPF will expand the variation range of grid impedance and enhance the stability of the system. The simulation results have verified the correctness of the theoretical analysis.

Index Terms: Low voltage ride-through, grid-connected inverters, instability, low-pass filter.

1 Introduction

As an interface circuit between wind power, photovoltaic power, and other power units with the power grid, the control performance of grid-connected inverters is crucial for the stable operation of the whole power system. Grid-connected inverters can be divided into grid-following (GFL) inverters and grid-forming (GFM) inverters. The former inverters are controlled as a controllable current source, while the latter are controlled as a controllable voltage source [1-3]. Due to their excellent active and reactive power decoupling ability and superior current limiting characteristics, GFL inverters are the mainstream solution and the backup scheme for GFM inverters during faults [4-5].

Short circuits, grounding faults, and other faults in the power system often lead to the voltage drop at the Point of Common Coupling (PCC) for renewable power systems [6]. The voltage-dip fault at the PCC may lead to undervoltage protection of the connected load and disconnection of the other power generation unit, threatening the stability of the whole system. To prevent such adverse consequences, the grid code requires that all inverters connected to the grid should have low-voltage-ride-through (LVRT) capability [7-9]. That is, the inverters need to maintain the grid-connection state for a period after faults and raise the PCC voltage by injecting reactive current into the grid. It is found that under this circumstance, the system may experience instability, especially under the weak grid. This phenomenon is different from the instability phenomenon caused by weak damping reported in previous literature [10].

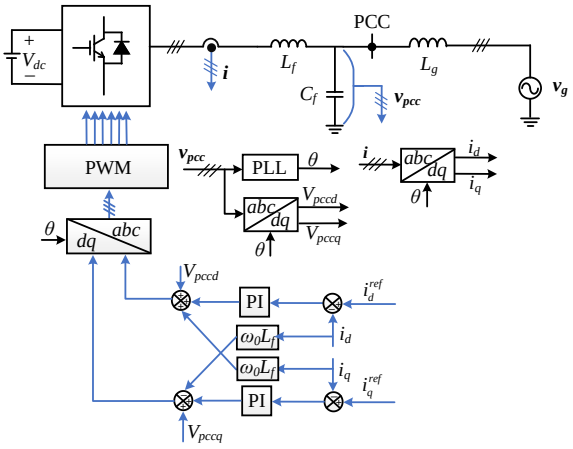

Fig.1 System diagram of grid-connected inverters.

The instability mechanism is analyzed in this paper and the corresponding solution is proposed, which are the main contribution of the paper. The verification simulations are performed to validate the theoretical analysis. Finally, the conclusion is provided at the end of the paper.

2 Simplified model and low-frequency oscillations of grid-connected inverters

Fig.1 shows the single-line diagram of a three-phase grid-connected inverter, where L_f and C_f constitute LC filters. L_g represents line impedance. V_g indicates the grid voltage, and i denotes the output current. V_{dc} and V_{pcc} represent the dc-side voltage and PCC voltage. θ,

generated from the phase-locked loop (PLL), represents the phase of the voltage.

I_d^{ref} and I_q^{ref} represent the active and reactive current reference of the system, respectively. According to the grid code [11], their expressions are:

$$I_d^{ref} = \begin{cases} I_{rate} & 0.9\text{p.u.} \le V_{pcc} \le 1.1\text{p.u} \\ (0.2 \sim 0.4) * I_{rate} & V_{pcc} < 0.9\text{p.u.} \end{cases}$$

$$I_q^{ref} = \begin{cases} 0 & 0.9\text{p.u.} \le V_{pcc} \le 1.1\text{p.u.} \\ k_{q\_adj} * (0.9 - V_{pcc}) * I_{rate} & V_{pcc} < 0.9\text{p.u.} \end{cases} \quad (1)$$

where, I_{rate} represents the rated output current of the system. $k_{q\text{-}adj}$ denotes the adjustment coefficient of reactive current during LVRT process, generally ranging from 1.5 to 2.5 [12].

As shown in Fig. 1, the PI controller is used with the current control loop to make the output current *i* to track its reference I_d^{ref} and I_q^{ref}. It is worth noting that this paper mainly studies the low-frequency oscillation of the system, and the cutoff frequency of LC filters is generally much higher than this frequency. Therefore, for simplification, the influence of LC filters is ignored in subsequent analysis.

3 Mechanism analysis and low-pass filter-based solution

3.1 Mechanism analysis

Usually, the control bandwidth of the current loop is much larger than the system frequency. Therefore, when analyzing low-frequency oscillations, the dynamics of the current control loop can be omitted. The simplified system model is shown in Fig. 2.

According to Fig. 2, the amplitude of PCC voltage can be expressed as:

$$\begin{gathered} V_{pcc} = V_g e^{-\mathrm{j}\delta} + (I_d^{ref} + \mathrm{j}I_q^{ref}) \cdot \mathrm{j}X_g \\ \Downarrow \\ V_{pccd} = V_g \cos(\delta) - I_q^{ref} X_g \\ V_{pccq} = -V_g \sin(\delta) + I_d^{ref} X_g \end{gathered} \quad (2)$$

where, V_{pccd} and V_{pccq} represent the d-axis and q-axi components of the PCC voltage after abc/dq transformation, respectively. δ is the phase difference between the PCC voltage and the grid voltage.

Due to that PLL will reduce the V_{pccq} to zero after the adjustment process, (2) can be further simplified as:

$$\begin{cases} V_{pccd} = \sqrt{V_g^{\,2} - (I_d^{ref} X_g)^2} - I_q^{ref} X_g \\ V_{pccq} = 0 \end{cases} \quad (3)$$

Then, the amplitude of the PCC voltage can be expressed as:

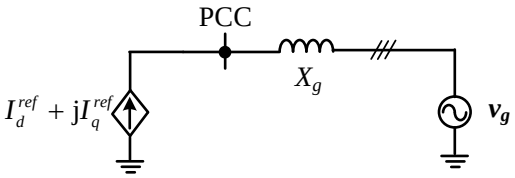

Fig. 2 Simplified diagram of the system.

$$V_{pcc} = V_{pccd} = \sqrt{V_g^{\,2} - (I_d^{ref} X_g)^2} - I_q^{ref} X_g \quad (4)$$

3.2 System stability analysis under grid code

After the voltage-dip fault, the grid-connected inverter is required to inject reactive current into the power grid according to the grid code in (1). The voltage amplitude at the PCC during the fault is:

$$\begin{aligned} V_{pcc}(n+1) = &\sqrt{V_g^{\,2} - (I_d^{ref} X_g)^2} \\ &+ k_{q\_adj}(0.9 - V_{pcc}(n)) X_g \end{aligned} \quad (5)$$

It is worth noting that the control strategy of grid-connected inverters is often implemented through interrupts in the controller. Here, V_{pcc} (n+1) and V_{pcc} (n) represent the PCC voltage at (n+1)T_s and nT_s moment. T_s is the switching period of the system.

According to (5), the steady-state PCC voltage after injecting reactive current is:

$$V_{pcc}^{\,*} = \frac{\sqrt{V_g^2 - (I_d^{ref} X_g)^2} + 0.9 k_{q\_adj} X_g}{1 + k_{q\_adj} X_g} \quad (6)$$

As long as $V_g > I_d^{ref} X_g$, the fixed point of V_{pcc} will exist during the LVRT process.

In addition to the existence of the fixed point, it is also necessary to ensure the stability of the fixed point so that the system can converge to it.

The fixed point can be defined by equation (7),

$$\begin{aligned} V_{pcc}^* &= f(V_{pcc}^*) \\ &= \sqrt{V_g^{\,2} - (I_d^{ref} X_g)^2} + k_{q\_adj}(0.9 - V_{pcc}^*) X_g \end{aligned} \quad (7)$$

To ensure the stability of the system, the following conditions should be met [13-14],

$$\left| \frac{\mathrm{d}f(V_{pcc}^*)}{\mathrm{d}V_{pcc}^*} \right| = k_{q\_adj} X_g < 1 \Rightarrow X_g < \frac{1}{k_{q\_adj}} \quad (8)$$

Therefore, under the same reactive current coefficient, the inverters may lose small-signal stability when the grid impedance violates the criterion in (8).

3.3 Low-pass-filter-based solution

As shown in section 3.2, during the LVRT process, the grid-connected inverters are prone to be unstable

under a weak grid. It is found in this paper that when a low-pass filter (LPF) used with the PCC voltage amplitude detection module can alleviate the instability. The detailed analysis is as follows.

When using the LPF, (5) will be changed to:

$$\begin{aligned} V_{pcc}(n+1) &= \sqrt{V_g^{\,2} - (I_d^{ref} X_g)^2} \\ &+ k_{q\_adj}(0.9 - V_{pcc}(n) * \frac{\omega_p}{\frac{z-1}{zT_s} + \omega_p}) X_g \\ &= H - k_{q\_adj} X_g V_{pcc}(n) * \frac{\omega_p}{\frac{z-1}{zT_s} + \omega_p} \end{aligned} \tag{9}$$

where, $\frac{\omega_p}{\frac{z-1}{zT} + \omega_p}$ is the discrete transfer function of the LPF and $H = \sqrt{V_g^2 - (I_d^{ref} X_g)^2} + 0.9 k_{q\_adj} X_g$.

(9) can be further simplified as:

$$(z + k_{q\_adj} X_g \frac{\omega_p}{\frac{z-1}{zT_s} + \omega_p}) V_{pcc}(z) = H \tag{10}$$

The characteristics equation of (10) is:

$$z + k_{q\_adj} X_g \frac{\omega_p}{\frac{z-1}{zT_s} + \omega_p} = 0 \tag{11}$$

To ensure the small-signal stability, the root of equation (11) needs to be located inside the unit circle leading to [15-16]:

$$\begin{aligned} & k_{q\_adj} X_g < \frac{2}{\omega_p T_s} + 1 \\ & \Downarrow \\ & X_g < \frac{1}{k_{q\_adj}} + \frac{2}{k_{q\_adj} \omega_p T_s} \end{aligned} \tag{12}$$

Comparing the results in (10) and (6), it can be obtained that the LPF can enlarge the range of grid impedance.

In practice, the maximum per unit value of line impedance X_g is 1.0 p.u. To ensure the stability of the whole system, the range of filter parameters is:

$$\begin{aligned} & 1.0 \le \frac{1}{k_{q\_adj}} + \frac{2}{k_{q\_adj} - 1} \\ & \Downarrow \\ & \omega_p T_s \le \frac{2}{k_{q\_adj} - 1} \end{aligned} \tag{13}$$

4 The configurable grid impedance range under the conventional scheme and the proposed scheme

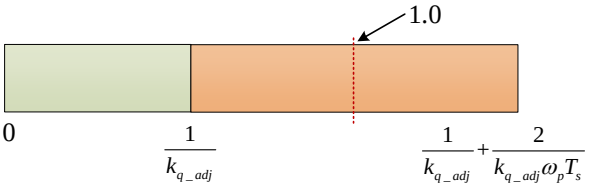

Fig. 3 The configurable parametric range of the grid impedance.

The configurable grid impedance under the conventional scheme and the proposed scheme is shown in Fig.3. Under the conventional scheme, the upper limit of the grid impedance X_g is $\frac{1}{k_{q\_adj}}$. With the proposed scheme, the upper limit of the grid impedance X_g can be increased to $\frac{1}{k_{q\_adj}} + \frac{2}{k_{q\_adj}\omega_p T_s}$. When the $\omega_p T_s$ is configured to be smaller than $\frac{2}{k_{q\_adj} - 1}$, the instability phenomenon can be thoroughly avoided. Under this condition, the grid-connected inverters will keep stable no matter how the grid impedance is adopted. Therefore, the proposed low-pass filter can expand the grid impedance range and enhance the stability of the system. This is the main contribution of the paper.

5 Simulation verification

To verify the effectiveness of the analysis, simulation tests are conducted, where the main parameters listed in Table I are used for the setup.

Tab. I Table of the system parameters

Symbol	Item	Value
V_g	Grid voltage (*l-l*, rms)	653V(1.0p.u.)
f_0	Rated frequency	50Hz
f_{sw}	Switching frequency	16kHz
L_f	Filter inductor	140μH
C_f	Filter capacitor	21μF
P_{ref}	Rated power	228kW
I_d^{ref}	Rated active current	233A
I_q^{ref}	Rated reactive current	0A
k_{q_adj}	Adjustment coefficient of reactive current	1.5
X_g	Line impedance	0.84Ω (0.30p.u.)

DOI:10.30420/566414094

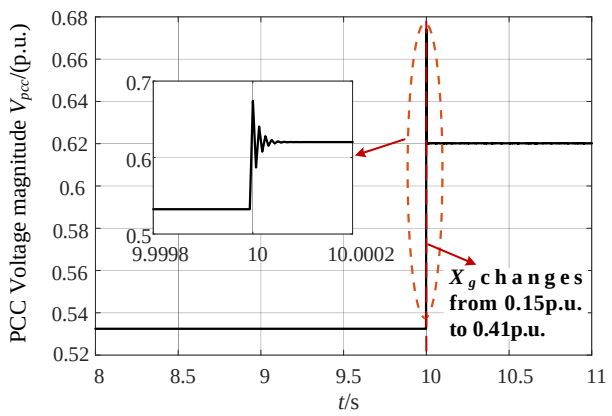

Fig. 4 The PCC voltage of grid-connected inverters during LVRT process when grid impedance changes from 0.15p.u. to 0.41p.u. and the adjustment coefficient of reactive current k_{qadj} keeps as 1.5.

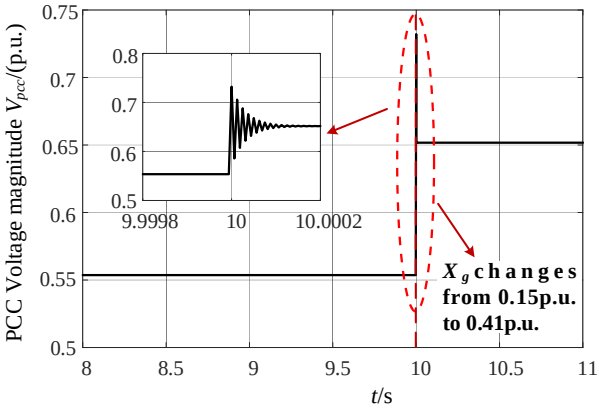

Fig. 5 The PCC voltage of grid-connected inverters during LVRT process when grid impedance changes from 0.15p.u. to 0.41p.u. and the adjustment coefficient of reactive current k_{qadj} keeps as 2.0.

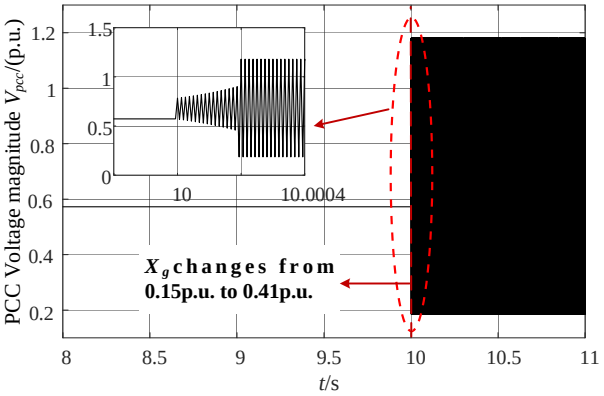

Fig. 6 The PCC voltage of grid-connected inverters during LVRT process when grid impedance changes from 0.15p.u. to 0.41p.u. and the adjustment coefficient of reactive current k_{qadj} keeps as 2.5.

The verification results are shown in Fig. 4-Fig. 10. From Fig. 4- Fig. 6, it is observed that the increase of the reactive current adjustment coefficient will lead to the instability of the system under the conventional

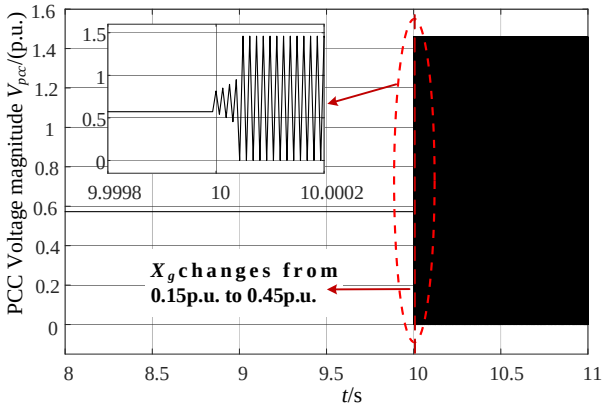

Fig. 7 The PCC voltage of grid-connected inverters during LVRT process when grid impedance changes from 0.15p.u. to 0.45p.u. and the adjustment coefficient of reactive current k_{qadj} keeps as 2.5.

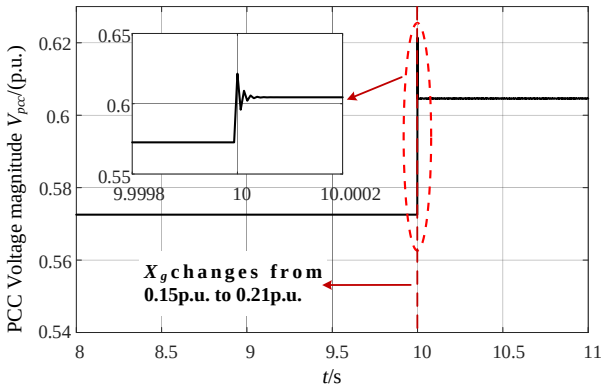

Fig. 8 The PCC voltage of grid-connected inverters during LVRT process when grid impedance changes from 0.15p.u. to 0.21p.u. and the adjustment coefficient of reactive current k_{qadj} keeps as 2.5.

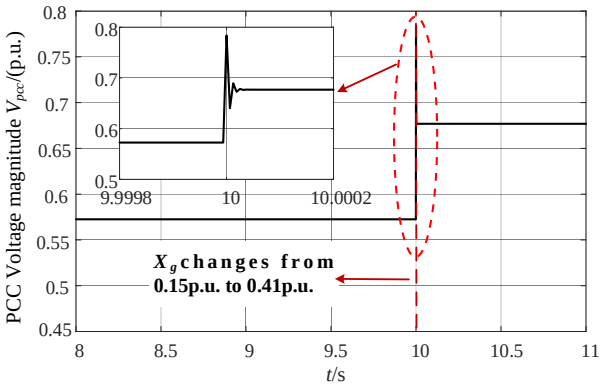

Fig. 9 The PCC voltage of grid-connected inverters during LVRT process when grid impedance changes from 0.15p.u. to 0.41p.u. and the adjustment coefficient of reactive current k_{qadj} keeps as 2.5 under the proposed scheme.

scheme. From Fig. 6-Fig. 8, it is observed that the increase of the grid impedance will lead to the instability of the system under the conventional scheme. This phenomenon is consistent with the theoretical analysis

ISBN 978-3-8007-6414-3

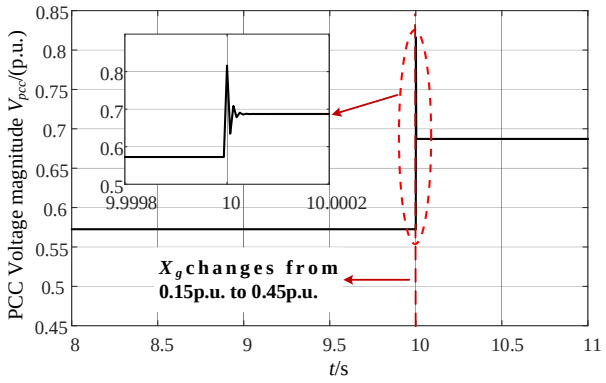

Fig. 10 The PCC voltage of grid-connected inverters during LVRT process when grid impedance changes from 0.15p.u. to 0.45p.u. and the adjustment coefficient of reactive current k_{qadj} keeps as 2.5 under the proposed scheme.

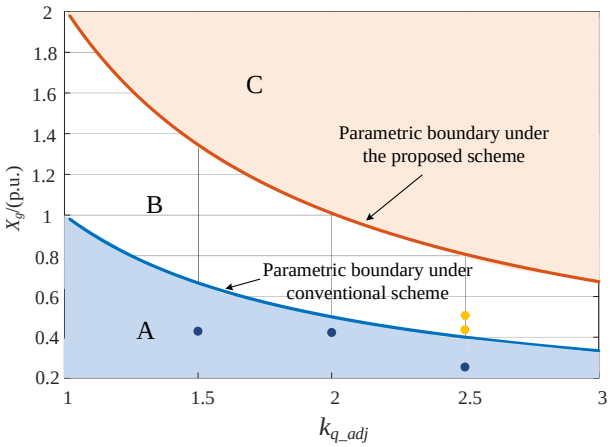

Fig. 11 The change of the parametric boundary under the conventional scheme and the proposed scheme(● represents the cases after verification).

in the stability criterion in section 3.2 that the grid impedance cannot be too large.

From Fig. 9-Fig. 10, it is observed that inverters under the proposed scheme can avoid instability with the same grid impedance and reactive current adjustment coefficient parameters.

A whole parametric boundary under the conventional scheme and the proposed scheme is shown in Fig. 11. The stable parametric range is area A under the conventional scheme. All the cases outside of A will be unstable, as shown in Fig. 6 and Fig. 7. Under the proposed scheme, the stable parametric area will expand from A to A+B. All the cases inside this area will be stable, as shown in Fig. 9 and Fig. 10. These results verify that the proposed scheme can enhance the stability of the inverters.

6 Conclusion

An instability phenomenon of grid-connected inverters caused by the large grid impedance is revealed and analyzed. The obtained verification results prove that the large impedance will make the characteristic roots move to the outside of the unit circle leading to instability. The proposed LPF used with the PCC voltage detection module can enlarge the configurable range of grid impedance leading to the enhancement of the stability performance.

References

[1] R. Rosso, X. Wang, M. Liserre, X. Lu and S. Engelken, “Grid-Forming Converters: Control Approaches, Grid-Synchronization, and Future Trends—A Review,” *IEEE Open J. Ind. Appl.*, vol. 2, pp. 93-109, Apr. 2021.

[2] X. Wang, F. Blaabjerg and W. Wu, “Modeling and Analysis of Harmonic Stability in an AC Power-Electronics-Based Power System,” *IEEE Trans. on Power Electron.*, vol. 29, no. 12, pp. 6421-6432, Dec. 2014.

[3] Pan D, Wang X, Liu F , et al. “Transient Stability of Voltage-Source Converters With Grid-Forming Control: A Design-Oriented Study,” *IEEE J. Emerg. Select. Topics Power Electron.* vol. 8, no. 2, pp. 1019-1033, Oct. 2019.

[4] F. Blaabjerg, R. Teodorescu, M. Liserre and A. V. Timbus, “Overview of Control and Grid Synchronization for Distributed Power Generation Systems,” *IEEE Trans. Ind. Electron.*, vol. 53, no. 5, pp. 1398-1409, Oct. 2006.

[5] E. Afshari et al., “Control Strategy for Three-Phase Grid-Connected PV Inverters Enabling Current Limitation Under Unbalanced Faults,” *IEEE Trans. Ind. Electron.*, vol. 64, no. 11, pp. 8908-8918, Nov. 2017.

[6] Kundur, *Power System Stability and Control*. New York, NY, USA: McGraw-Hill, 1994.

[7] Teodorescu, Remus, M. Liserre, and P. Rodriguez. *Grid Converters for Photovoltaic and Wind Power Systems*. Wiley, 2011.

[8] IEEE Standard 929. IEEE Recommended Practice for Utility Interface of Photovoltaic (PV) Systems, IEEE: Piscataway, NJ, USA, 2000.

[9] IEEE Standard 1547. IEEE Standard for Interconnecting Distributed Resources with Electric Power Systems, IEEE: Piscataway, NJ, USA, 2003.

[10] Wu H and Wang X. *An Adaptive Phase-Locked Loop for the Transient Stability Enhancement of Grid-Connected Voltage Source Converters*, 2018 IEEE Energy Conversion Congress and Exposition (ECCE), OR, USA, 2018: 5892-5898.

[11] The State Administration for Market Regulation of China. *Technical requirements for photovoltaic grid-connected inverter: GB/T 37408-2019*, 2019.

[12] The State Administration for Market Regulation *Technical regulations for connecting photovoltaic power stations to power systems*: *GB/T* 19964-2012, 2012.

[13] Slotine, Jean-Jacques E., and Weiping Li. *Applied nonlinear control*. Vol. 199. No. 1. Englewood Cliffs, NJ: Prentice hall, 1991.
[14] S. H. Strogatz, *Nonlinear Dynamics and Chaos: With Applications to Physics, Biology, Chemistry, and Engineering*. New York, NY, USA: Perseus Books, 1994.
[15] Cheb-Terrab, E. S., and H. P. De Oliveira. “Poincaré sections of Hamiltonian systems.” *Computer physics communications* 95.2-3 (1996): 171-189.
[16] Yuri A.Kuznetsov, *Elements of Applied Bifurcation Theory*, New York, NY, USA: Springer-Verlag, 2004.